(Received 21 October 2024, Accepted 12 December 2024, Scheduled 11 January 2025)

A Low-Cost Four Circularly Polarized Antenna Loaded with a Complementary Split Ring Resonator for Beam Steering Applications

Oumaima Nayat-Ali*, Fatima Z. Khoutar, Mariem Aznabet, Otman EL Mrabet, and Mohsine Khalladi

Intelligent System Design Laboratory (ISD), Faculty of Science, Abdelmalek Essaadi University, Tetuan 93000, Morocco

ABSTRACT: In this work, a novel circularly polarized antenna with four ports and loaded with complementary split ring resonator (CSRR) for beam steering applications without phase shifters or PIN diodes is presented. The single antenna loaded with CSRR is arranged in a rotational manner forming a 4-port structure. The separation distance among the four antennas is optimized for achieving a steering angle of 28° with an isolation level greater than 25 dB over the whole bandwidth. When one of the four antennas is excited, the others either open-circuited or terminated to a 50-Ω impedance, the antenna has a resonant frequency of 5.8 GHz and produces a left-hand circularly polarized (LHCP) tilted beam in the elevation plane. The introduction of the CSRR leads to achieving a small design and also to get circular polarization characteristics. The proposed structure has a radiation efficiency of 90% and a gain of 6 dBi over the whole bandwidth. This characteristic can be tuned which makes the proposed design suitable for many modern communication systems.

1. INTRODUCTION

Antennas with beam steering capability have gained a lot of interest during the last decade and are being widely used in satellite communications, weather surveillance radars, and military radar systems owing to their ability to tackle many problems that wireless communications can suffer nowadays [1–3]. For example, the use of those antennas can solve the problem of interference/noise, increasing the data rate transmission. One of the most straightforward methods for beam steering involves the use of phased array antenna [4]. Nevertheless, despite their numerous advantages, including high gain and beam control, phased array antennas do exhibit certain limitations. These limitations encompass the need for a substantial number of radiating elements, resulting in bulkiness, increased costs due to power dividers and phase shifters, and overall complexity [5]. Consequently, these factors render phased array antennas unsuitable for use in modern mobile and portable communication systems. Therefore, these drawbacks have urged many researchers to explore other solutions that have the advantage of a small size and low cost. One interesting approach that has been proposed is called briefly ESPAR which refers to electronically steerable passive array radiator. This approach has the feature of achieving beam steering capability without relying on the use of phase shifters, which makes it very attractive [6–12]. This type of antenna is composed of a single driven antenna surrounded by closely spaced parasitic elements loaded with reactive loads. Owing to mutual coupling, the parasitic elements can be excited, and by controlling the reactance, the beam can be directed in a specific direction. Other approaches that have gained much attention more recently rely on the use of a single element antenna to achieve beam steering capability by modifying the antenna current path using either PIN diodes [13], microelectromechanical system switches (MEMS) [14], or photoconductive switches [15]. Another intriguing method based on the use of gradient index lenses fabricated using 3D printing is also being investigated to get beam steering antennas [16, 17]. This method's primary benefit is that lens antennas are often used for beam steering applications due to their high gain and capacity to concentrate electromagnetic waves in certain directions. The use of liquid antennas, particularly those based on salty and pure water, offers an interesting approach for beam-steering applications [18]. For example, in [19], the authors present a salty water antenna with 360° beam-steering capabilities, combining the concepts of an electronically steerable parasitic array radiator (ESPAR) antenna and a water-based antenna. To the best of our knowledge, the majority of the developed mentioned antennas with beam steering capability are linearly polarized. This feature limits their applications in modern communications systems, such as satellite communications or weather surveillance due to the reasons discussed at the beginning of the introduction section.

In this paper, a novel, compact, and low-cost design featuring four circularly polarized antennas, each loaded with a complementary split ring resonator (CSRR) and equipped with four feeds to enable beam steering capability, is presented for the first time. The beam steering capability was achieved without the use of phase shifters or PIN diodes. The proposed structure operates at 5.8 GHz and exhibits a gain of 6 dBi. The introduction of a CSRR into the antenna not only reduces antenna size but also enable producing circular polarization. However,

* Corresponding author: Oumaima Nayat-Ali (oumaima.nayatali@gmail.com).

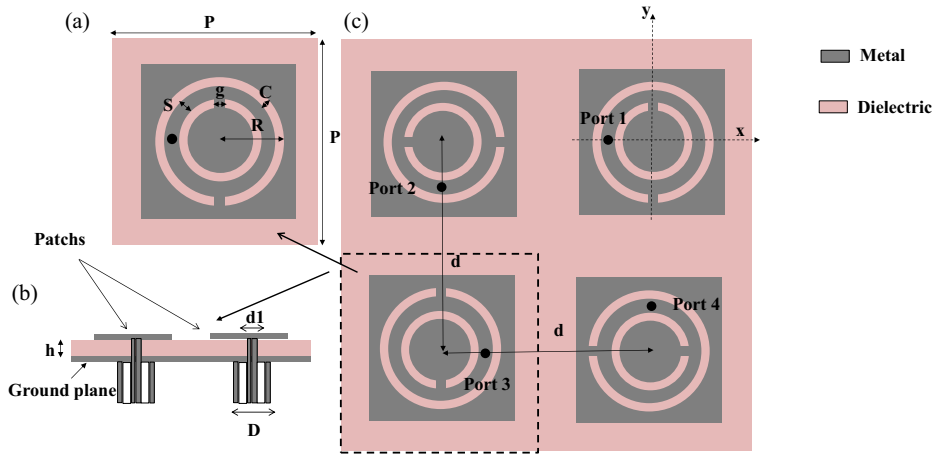

FIGURE 1. Geometry of proposed beam steering antenna array with CP: (a) Single antenna, (b) Side view, (c) Front view.

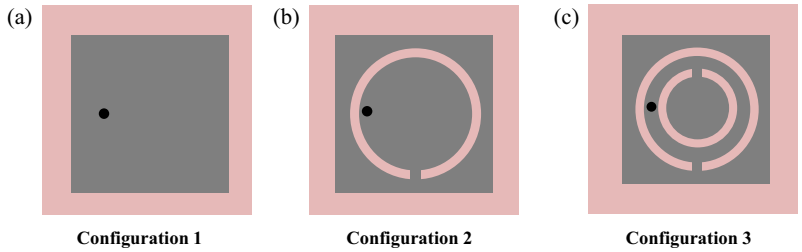

FIGURE 2. The evolution of the proposed CP antenna.

the beam steering capability is originated from the mutual coupling with other antennas. The separation distance among the four antennas is optimized for achieving a steering angle of 28° with an isolation level greater than 25 dB over the whole bandwidth.

2. ANTENNA DESIGN AND ANALYSIS

The proposed structure is composed of four square loaded CSRR patch antennas placed in a rotational symmetry, sharing the same ground plane and occupying an overall size of $50 \times 50 \times 1.527\,\text{mm}^3$ as shown in Fig. 1. This structure has been optimized to have a resonant frequency around 5.8 GHz.

The radiating elements are printed on the top of a dielectric substrate RO3003 having a dielectric permittivity constant of 3, loss tangent of 0.001, and thickness of 1.52 mm. The dimension of a single square antenna is $25 \times 25\,\text{mm}^2$.

The CSRR has the following dimensions: the radius of outer slot ring is $R = 3\,\text{mm}$. The separation distance between the inner and outer slot rings is $S = 1.4\,\text{mm}$. The width of slots is $C = 0.5\,\text{mm}$, and the anti-gap length is 0.4 mm. In this study, loading the square patch antenna with a CSRR plays an important role in achieving circular polarization and enhancing beam steering tilt angle.

Each antenna is excited separately by an SMA connector creating a 4-port configuration. The separation distance among the four antennas is optimized for achieving high isolation and broadens the scope of beam scanning capability. When a single one of these antennas is excited while the others are terminated with 50-Ω, the antenna radiates with a tilted beam in the elevation plane. The excited antenna acts as a driven structure, and it establishes parasitic coupling with the other three antennas, which act as parasitic elements. The latter are excited through the generation of surface and lateral waves by the primary driven antenna. Note that compared to other ESPARs configurations published in the literature, this work removes the necessity for diodes and costly phase shifters leading to a notable decrease in both cost and fabrication complexity. To study the main characteristic of the proposed structure, CST Microwave Studio, particularly time domain solver, was used. To explain the design development process as shown in Fig. 2. We have started by simulating a conventional square microstrip (configuration 1) to achieve good impedance matching around the resonant frequency 5.8 GHz. Then, we have introduced a single circular slot with an anti-gap as shown in Fig. 2(b). The idea is to reduce the dimension of the first configuration and to achieve circular polarization characteristics. The latter has been optimized in the case of the introduction of a complementary split ring resonator (CSRR) as shown in Fig. 2(c) with a reduced size (Configuration 3). The reflection coefficients and axial ratios of three configurations are plotted in Fig. 3.

From Fig. 3, it is evident that all configurations have the same resonant frequency. However, the third configuration stands out for its smaller size and enhanced circular polarization characteristics. In contrast, the first configuration acts as a linearly polarized antenna.

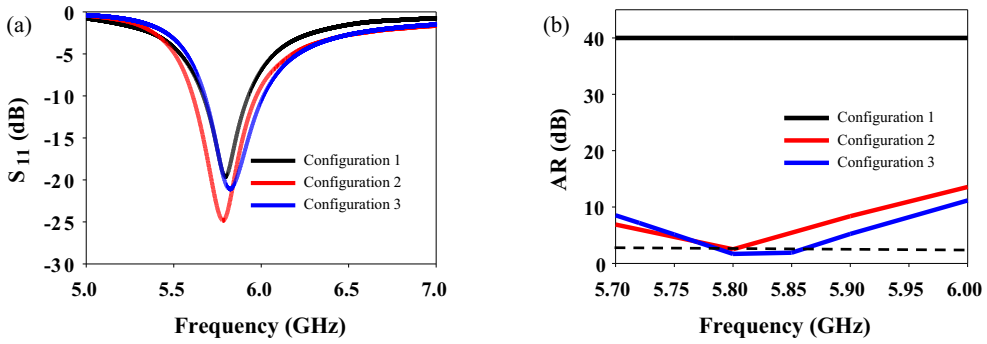

FIGURE 3. (a) Reflection Coefficient and (b) Axial ratio of the three configurations as a function of frequency.

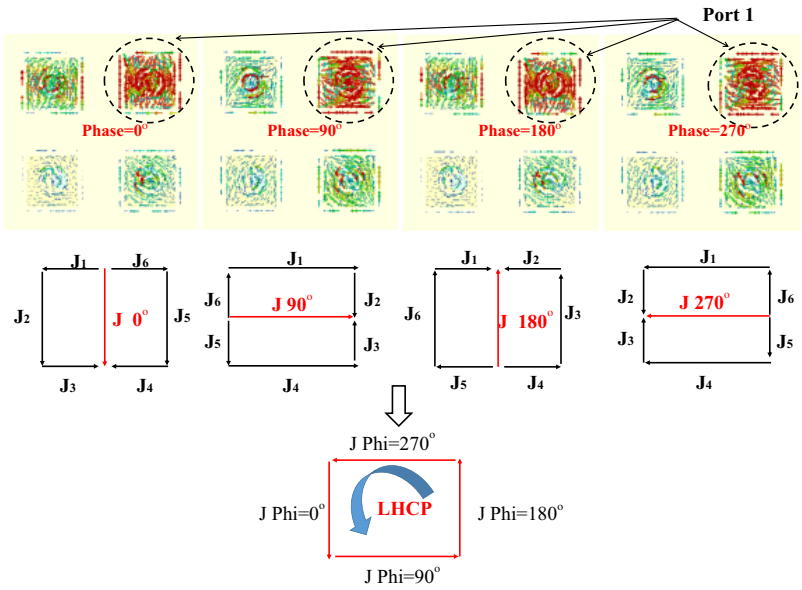

FIGURE 4. Current distribution at Port 1.

The simulated surface current distributions of the proposed CP array antenna at different feeding phases are shown in Fig. 4. These are 0°, 90°, 180°, and 270° for port 1.

To clarify the operating principle of the CP antenna, the vector current distributions on the patch and around CSRR were examined. The surface currents are uniformly distributed, with maximum intensity on the patch and CSRR of each element. These distributions are presented over a period corresponding to a frequency of 5.8 GHz.

The current paths are designated by J_1 to J_6. At a phase of 0°, J_1, J_2, J_3, J_4, J_5, and J_6 mainly contribute to the surface current distribution, with currents in J_6 and J_4 being cancelled out by those in J_1 and J_3. Then, at 0°, J_2 and J_5 are primarily responsible for directing the current in the $-y$ direction, whereas at 90°, J_1, J_2, J_3, J_4, J_5, and J_6 are primarily responsible for directing the surface current distribution seen in Fig. 4. In J_3 and J_6, the surface current in the y direction cancels out that in J_2 and J_5. The 90° phase surface is then primarily pointed in the x direction by J_1 and J_4. Additionally, the current direction shifts to the $+y$ direction at 180° and then back to the $-x$ direction at 270°. The magnitudes of the current vectors at 0° and 90° are similar to those at 180° and 270°, with opposite phase orientations. The figure clearly shows an anticlockwise wave progression with a changing phase, confirming the generation of circularly polarized radiation. Consequently, a left-hand circularly polarized (LHCP) wave in the $+z$ direction is achieved.

Figure 5 shows the simulated 3D radiation pattern at 5.8 GHz.

3. FABRICATION, MEASUREMENTS AND DISCUSSION

The proposed structure is fabricated and measured to validate the design approach. A photograph of fabricated antenna is shown in Fig. 6. This structure has been fabricated using an LPKF Protomat S100 mill/drill unit machine controlled via a computer.

Measurements of the S-parameters for the proposed structure were conducted using an Agilent N5234B PNA-L network analyzer, and the obtained results are presented in Fig. 7(a). The measured and simulated results demonstrate good impedance

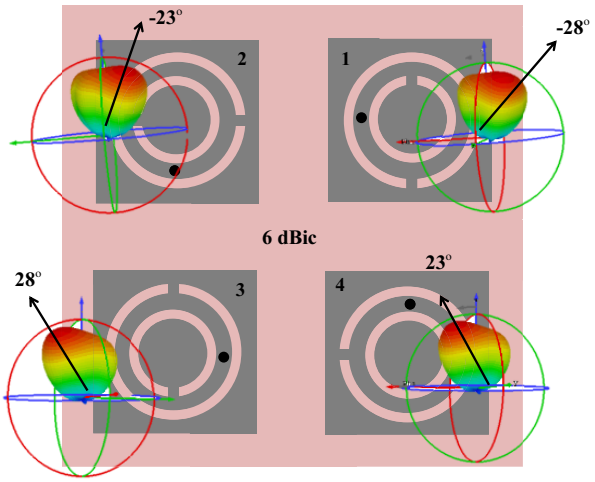

FIGURE 5. Simulated 3D radiation pattern of the proposed antenna with different port excitation.

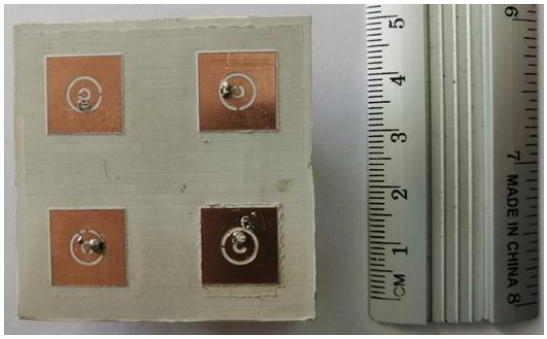

FIGURE 6. Photo of the fabricated structure.

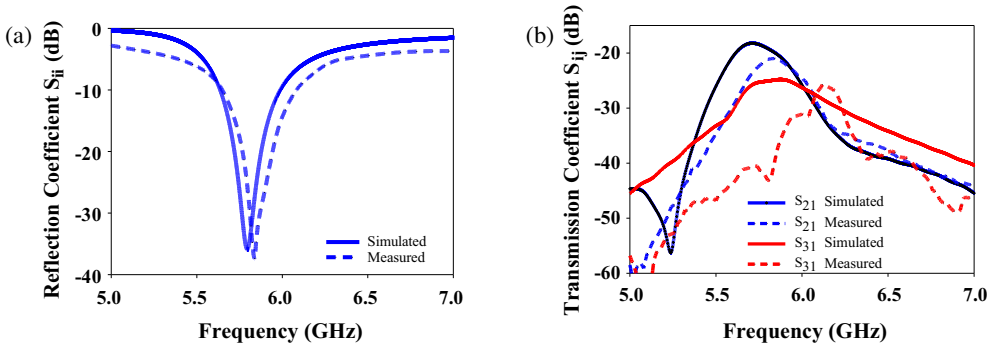

FIGURE 7. Measured and simulated S-parameters of the proposed structure: (a) S_{11}; (b) S_{21}, S_{31}, and S_{41}.

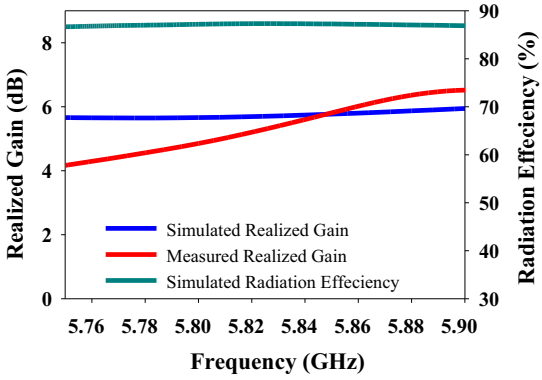

FIGURE 8. Measured and Simulated realized Gain, and Simulated radiation efficiency.

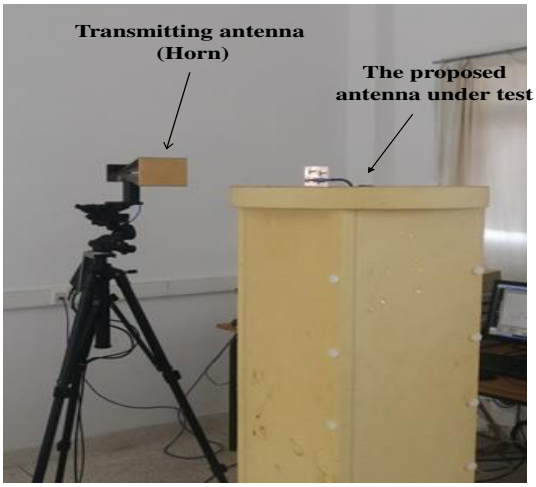

FIGURE 9. Measured setup used to measure radiation patterns.

matching, with a reflection coefficient (S_{11}) below -10 dB between 5.6 and 5.9 GHz. To be concise, the measured reflection coefficients (S_{11}) of the other antennas not shown here matched well with the one presented in Fig. 7(a), owing to the symmetrical arrangement of the four antennas.

Figure 7(b) illustrates that the mutual couplings among the four antennas when one is excited are small which are less than -20 dB over the whole bandwidth.

Next, we have measured the realized gain which is presented in Fig. 8. We can see clearly that the loaded antenna with a CSRR provides a gain of more than 6 dBi over the whole bandwidth, and the radiation efficiency is close to 90%.

To experimentally demonstrate the capability of the proposed structure, which consists of 4 circularly polarized antennas pro-

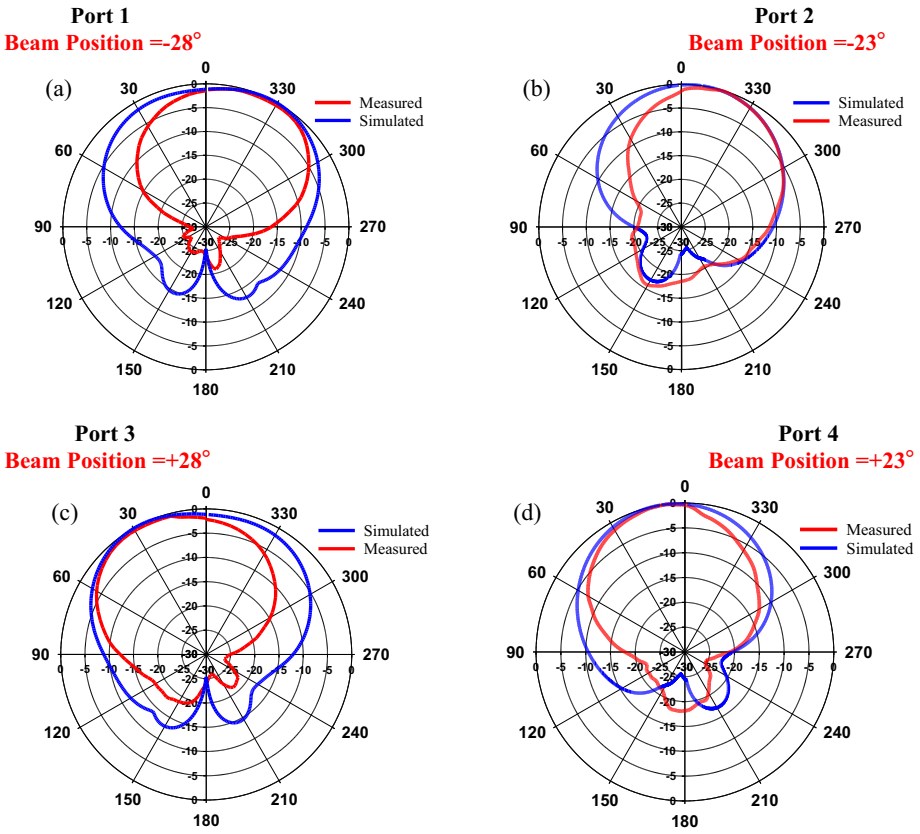

FIGURE 10. 2D Measured and simulated radiation patterns of four antennas at 5.8 GHz.

TABLE 1. Comparison of the proposed beam steering antenna with other similar published antennas.

Reference	Number of substrate	Beam tilt angle (°)	Peak Gain (dB)	Polarization	Method	Size (λ)
[12]	3	37°	8	LP	Varactor Diodes	$1.4\lambda \times 1\lambda \times 0.037\lambda$
[21]	1	30°	6	LP	Change feed ports	$0.8\lambda \times 0.8\lambda \times 0.012\lambda$
[22]	1	27°	7	LP	Combination of reconfigurable parasitic patches	$0.98\lambda \times 0.74\lambda \times 0.07\lambda$
[23]	1	24°	6	LP	PIN diodes	$0.56\lambda \times 0.56\lambda \times 0.012\lambda$
[24]	2	28°	7	LP	Varactor Diodes	$0.7\lambda \times 0.7\lambda \times 0.083\lambda$
This work	1	28°	6	CP	Change position of port	$0.48\lambda \times 0.48\lambda \times 0.003\lambda$

viding beam steering characteristics, we measured their 2D radiation patterns corresponding to the elevation plane at the resonant frequency of 5.8 GHz. Here, we have used a UWB system for Time-Domain Near-Field Antenna Measurement developed by Geozondas [20], as shown in Fig. 9.

The obtained results, illustrating the 2D radiation patterns, are presented in Fig. 10. A significant level of agreement is observed when comparing the measured results with the simulated ones. It is evident that main beam direction changes with the proper choice of the port or the antenna. Specifically, the main radiated beam of the structure is steered by $-28°$ with a peak gain of 5.77 dBi when port 1 is excited. Port 2 excitation results in a maximum peak direction of 5.77 dBi, and the radiated beam can be steered by $-23°$. The structure successfully achieves a steer of $+23°$ with a gain of 5.77 dBi when port 4 is excited. As depicted in Fig. 10, a beam steering of 28° with a gain of 5.77 dBi was achieved when port 3 was excited.

The beamsteering capability can be obtained by controlling the coupling between the driven and parasitic elements. This coupling is influenced by both the distance and orientation relative to the driven element. The closer the parasitic components are, the greater the current flow through them.

It is noteworthy that tilting the beam did not affect the gain. Furthermore, the tilting angles could be potentially increased

by integrating a varactor diode to load each parasitic element, allowing precise control over the required phase shift for beam steering. This approach could be explored in future research.

A detailed comparison of our antenna with previously reported designs, focusing on beams numbers, angle tilt, gain, number of substrates, polarization type, and the beam-steering method, is presented in Table 1. We can see clearly that our design presents numerous features like minimum overall size and circular capability compared to the papers presented in Table 1.

4. CONCLUSION

This paper details the development, simulation, fabrication, and testing of a circularly polarized structure with beam steering capability operating at 5.8 GHz. The proposed design boasts several advantages, including satisfactory gain, acceptable half-power beamwidth, high efficiency, wide bandwidth, circular polarization enabled by a Complementary Split Ring Resonator (CSRR), and the ability to steer the beam in four directions. The latter functionality is achieved without the necessity of an additional phase shifters, varactor diodes or PIN diodes for switching, making the feed network simple and low cost. The proposed design holds promise for applications in MIMO technology, radar communications, and various wireless scenarios.

REFERENCES

[1] Zhou, H., A. Pal, A. Mehta, D. Mirshekar-Syahkal, and H. Nakano, "A four-arm circularly polarized high-gain high-tilt beam curl antenna for beam steering applications," *IEEE Antennas and Wireless Propagation Letters*, Vol. 17, No. 6, 1034–1038, Jun. 2018.

[2] Zhang, H., Y. Mahe, and T. Razban, "Low-cost Ku-band dual-polarized and beam switchable cross-type antenna array for satellite communications," *Microwave and Optical Technology Letters*, Vol. 56, No. 11, 2656–2659, 2014.

[3] Wang, X. and E. Aboutanios, "Theoretical analysis of reconfigurable adaptive antenna array in GNSS applications," in *21st European Signal Processing Conference (EUSIPCO 2013)*, 1–5, Marrakech, Morocco, Sep. 2013.

[4] Mailloux, R. J., *Phased Array Antenna Handbook*, 3rd ed., Artech House, 2017.

[5] Zhang, S., X. Chen, I. Syrytsin, and G. F. Pedersen, "A planar switchable 3-D-coverage phased array antenna and its user effects for 28-GHz mobile terminal applications," *IEEE Transactions on Antennas and Propagation*, Vol. 65, No. 12, 6413–6421, 2017.

[6] Harrington, R., "Reactively controlled directive arrays," *IEEE Transactions on Antennas and Propagation*, Vol. 26, No. 3, 390–395, May 1978.

[7] Kawakami, H. and T. Ohira, "Electrically steerable passive array radiator (ESPAR) antennas," *IEEE Antennas and Propagation Magazine*, Vol. 47, No. 2, 43–50, Apr. 2005.

[8] Yusuf, Y. and X. Gong, "A low-cost patch antenna phased array with analog beam steering using mutual coupling and reactive loading," *IEEE Antennas and Wireless Propagation Letters*, Vol. 7, 81–84, 2008.

[9] Nikkhah, M. R., J. Rashed-Mohassel, and A. A. Kishk, "Compact low-cost phased array of dielectric resonator antenna using parasitic elements and capacitor loading," *IEEE Transactions on Antennas and Propagation*, Vol. 61, No. 4, 2318–2321, Apr. 2013.

[10] Nikkhah, M. R., P. Loghmannia, J. Rashed-Mohassel, and A. A. Kishk, "Theory of ESPAR design with their implementation in large arrays," *IEEE Transactions on Antennas and Propagation*, Vol. 62, No. 6, 3359–3364, Jun. 2014.

[11] Movahedinia, R., M. R. Chaharmir, A. R. Sebak, M. R. Nikkhah, and A. A. Kishk, "Realization of large dielectric resonator antenna ESPAR," *IEEE Transactions on Antennas and Propagation*, Vol. 65, No. 7, 3744–3749, Jul. 2017.

[12] De Marco, R., E. Arnieri, G. Amendola, and L. Boccia, "Microstrip ESPAR antenna with conical beam scanning," *IEEE Antennas and Wireless Propagation Letters*, Vol. 23, No. 1, 174–178, 2023.

[13] Alam, M. S. and A. M. Abbosh, "Beam-steerable planar antenna using circular disc and four PIN-controlled tapered stubs for WiMAX and WLAN applications," *IEEE Antennas and Wireless Propagation Letters*, Vol. 15, 980–983, 2015.

[14] Cheng, S., P. Rantakari, R. Malmqvist, C. Samuelsson, T. Vaha-Heikkila, A. Rydberg, and J. Varis, "Switched beam antenna based on RF MEMS SPDT switch on quartz substrate," *IEEE Antennas and Wireless Propagation Letters*, Vol. 8, 383–386, 2009.

[15] Panagamuwa, C. J., A. Chauraya, and J. C. Vardaxoglou, "Frequency and beam reconfigurable antenna using photoconducting switches," *IEEE Transactions on Antennas and Propagation*, Vol. 54, No. 2, 449–454, Feb. 2006.

[16] Jia, D., Y. He, N. Ding, J. Zhou, B. Du, and W. Zhang, "Beam-steering flat lens antenna based on multilayer gradient index metamaterials," *IEEE Antennas and Wireless Propagation Letters*, Vol. 17, No. 8, 1510–1514, Aug. 2018.

[17] Giddens, H., A. S. Andy, and Y. Hao, "Multimaterial 3-D printed compressed Luneburg lens for mm-Wave beam steering," *IEEE Antennas and Wireless Propagation Letters*, Vol. 20, No. 11, 2166–2170, Nov. 2021.

[18] Huang, Y., L. Xing, C. Song, S. Wang, and F. Elhouni, "Liquid antennas: Past, present and future," *IEEE Open Journal of Antennas and Propagation*, Vol. 2, 473–487, 2021.

[19] Xing, L., J. Zhu, Q. Xu, D. Yan, and Y. Zhao, "A circular beam-steering antenna with parasitic water reflectors," *IEEE Antennas and Wireless Propagation Letters*, Vol. 18, No. 10, 2140–2144, Oct. 2019.

[20] Levitas, B., M. Drozdov, I. Naidionova, S. Jefremov, S. Malyshev, and A. Chizh, "UWB system for time-domain near-field antenna measurement," Geozondas Ltd. [Online]. Available: https://geozondas.com/pdf/UWB_system_for_time-domain_near-field_antenna_measurement.pdf.

[21] Pal, A., A. Mehta, D. Mirshekar-Syahkal, and H. Nakano, "A twelve-beam steering low-profile patch antenna with shorting vias for vehicular applications," *IEEE Transactions on Antennas and Propagation*, Vol. 65, No. 8, 3905–3912, Aug. 2017.

[22] Liu, C., Y. Cao, D. Yang, X. Yang, and Y. Chen, "Dual-polarized beam-switching yagi-uda patch antenna with large tilted angle," *Microwave and Optical Technology Letters*, Vol. 63, No. 5, 1445–1451, 2021.

[23] Fatemi-Nasab, J., S. Jarchi, and A. Keshtkar, "Complementary split ring resonator effects on radiation pattern reconfigurable circular microstrip antennas," *Iranian Journal of Electrical & Electronic Engineering*, Vol. 17, No. 1, 1775–1775, 2021.

[24] Bai, Y.-Y., S. Xiao, C. Liu, X. Shuai, and B.-Z. Wang, "Design of pattern reconfigurable antennas based on a two-element dipole array model," *IEEE Transactions on Antennas and Propagation*, Vol. 61, No. 9, 4867–4871, 2013.